CPC(HEP & NP), 2010, **34**(6): 842–847 Chinese Physics C Vol. 34, No. 6, Jun., 2010

Isospin violating mechanisms in quarkonium hadronic decays*

LI Gang(李刚)[1,3] ZHANG Yuan-Jiang(张远江)[1] ZHAO Qiang(赵强)[1,2] ZOU Bing-Song(邹冰松)[1,2]

[1] Institute of High Energy Physics, Chinese Academy of Sciences, Beijing 100049, China
[2] Theoretical Physics Center for Science Facilities, Chinese Academy of Sciences, Beijing 100049, China
[3] Department of Physics, Qufu Normal University, Qufu 273165, China

Abstract We analyze the ϕ meson production in $e^+e^- \to \omega\pi^0$ as a probe for studying the isospin violation mechanisms. By clarifying the dynamic sources causing the isospin violation, we succeed in quantifying those mechanisms with the help of the recent KLOE data. Hence, the $\phi \to \omega\pi^0$ branching ratio is extracted. We find that apart from the electromagnetic (EM) transitions, the strong transition via intermediate kaon loops plays an important role in understanding the cross section and its lineshape.

Key words Isospin violation, Intermediate meson loop

PACS 12.40.Vv, 13.20.Gd, 13.25.-k

1 Introduction

The e^+e^- annihilation below the charmonium threshold is a major source of information on the properties of light vector mesons (ρ, ω, ϕ) and their excited states. KLOE collaboration at the ϕ factory recently report the cross sections of $e^+e^- \to \omega\pi^0$ in the vicinity of the ϕ meson [1, 2]. With tiny experimental errors, the ϕ excitation appears as a dip at the ϕ mass, while the background contributions are smooth and flat. Since the reaction $e^+e^- \to \omega\pi^0$ is dominated by the $I=1$ transition matrix element, the interferences due to the ϕ $(I=0)$ production will provide an opportunity for probing the isospin-violating mechanism and its correlation with the Okubo-Zweig-Iizuka (OZI) rule [3].

The study of $\phi \to \omega\pi^0$ has been a long history. This isospin-violating transition is correlated with the OZI-rule violation if the ϕ and ω are indeed ideal mixtures between the flavor singlet and octet. As we have known, the isospin violation generally have two sources. One is the electromagnetic (EM) transition, and the other is strong transition arising from the mass difference between the u and d quark. This will cause nonvanishing transitions between isospin eigen states with $I=1$ and $I=0$. In this sense, the state mixing is correlated with the coupled channel transition. In early studies, mechanisms involving the π-η mixing or empirical ϕ-ω-ρ^0 mixing were explored [4–9]. In our case, we distinguish the state mixing and intermediate meson loop transitions based on an effective Lagrangian approach. It can be understood as factorizing out the transition mechanisms in a different way. We can then explicitly calculate the transition amplitudes with constraints from independent processes [10, 11]. As a consequence, the state mixings can also be examined.

As follows, we first analyze the transition mechanisms and introduce the effective Lagrangian framework. In Sec. 3, calculation results are presented and compared with the experimental data. In Sec. 4, we draw conclusions and a brief summary is given.

2 Theory construction

Notice that the leading contributions to $e^+e^- \to \omega\pi^0$ are from the single photon transitions. Thus, the transition amplitude will be a product of the EM current and an anti-symmetric tensor. Taking the advantage for the single Lorentz structure for the VVP coupling, we can factorize the total amplitude into

Received 26 January 2010

* Supported by National Natural Science Foundation of China (10675131, 10491306, 10435080, 10521003), Chinese Academy of Sciences (KJCX3-SYW-N2) and the Ministry of Science and Technology of China (2009CB825200)

the following expression:

$$\mathcal{M}_{fi}=\mathcal{M}_{fi}^{I=1}+\mathcal{M}_{fi}^{I=0}, \quad (1)$$

with

$$\mathcal{M}_{fi}^{I=0} = \mathcal{M}_{fi}^{\text{EM}-I=0}+ \mathrm{e}^{\mathrm{i}\delta_L}(\mathcal{M}_{fi}^{\text{Loop}-I=0}+\mathcal{M}_{fi}^{\text{mixing}-I=0}), \quad (2)$$

where $\mathcal{M}_{fi}^{I=1}$ and $\mathcal{M}_{fi}^{I=0}$ denote the isospin 1 and 0 component in the amplitude, respectively. The isospin 0 amplitude can be further factorized into EM and strong part, while the latter receives contributions from the intermediate meson loop transitions and states mixings. δ_L is the phase angle for the EM and loop transition amplitudes, which will be determined by the experimental data. The relative phase between $\mathcal{M}_{fi}^{\text{Loop}-I=0}$ and $\mathcal{M}_{fi}^{\text{mixing}-I=0}$ is given by the effective Lagrangian.

As follows, we present those amplitude components in detail.

2.1 $I=1$ transitions in VMD model

The $I=1$ component plays a role as background in respect to the ϕ meson excitation in $e^+e^-\to\omega\pi^0$. Around the ϕ mass region, the dominant contributions are due to the low-lying $I=1$ vector mesons, such as ρ^0, $\rho'(1450)$, etc. According to PDG [12], these two states are the nearest to ϕ, thus, would be the major contributing states. Their amplitudes can be expressed as follows in terms of VMD [13]:

$$\mathcal{M}_{fi}^{a} = \bar{v}^{(s')}(p_e')(-\mathrm{i}e\gamma^\beta)u^s(p_e)\frac{-1}{s(s-M_\rho^2+\mathrm{i}\Gamma_\rho(s)\sqrt{s})}\frac{eM_\rho^2}{f_\rho}\frac{g_{\omega\rho\pi}}{M_\omega}\varepsilon_{\alpha\beta\mu\nu}p_\rho^\alpha p_\omega^\mu\varepsilon_\omega^\nu, \quad (3)$$

$$\mathcal{M}_{fi}^{b} = \bar{v}^{(s')}(p_e')(-\mathrm{i}e\gamma^\beta)u^s(p_e)\frac{-1}{s(s-M_{\rho'}^2+\mathrm{i}\Gamma_{\rho'}(s)\sqrt{s})}\frac{eM_{\rho'}^2}{f_{\rho'}}\frac{g_{\omega\rho'\pi}}{M_{\rho'}}\varepsilon_{\alpha\beta\mu\nu}p_{\rho'}^\alpha p_\omega^\mu\varepsilon_\omega^\nu, \quad (4)$$

where eM_V^2/f_V is a direct photon-vector-meson coupling and $g_{\omega\rho\pi}$ and $g_{\omega\rho'\pi}$ are the VVP strong coupling constants. $\Gamma_\rho(s)$ and $\Gamma_{\rho'}(s)$ are energy-dependent total widths for the intermediate ρ and ρ', respectively. They are described by the two major decay modes, $\pi^+\pi^-$ and $\omega\pi^0$ [14]:

$$\Gamma_\rho(s) = \Gamma_\rho(M_\rho^2)\frac{M_\rho^2}{s}\left(\frac{p_\pi(s)}{p_\pi(M_\rho^2)}\right)^3+ \frac{g_{\omega\rho\pi}^2}{12\pi M_\omega^2}p_\omega^3(s), \quad (5)$$

$$\Gamma_{\rho'}(s) = \Gamma_{\rho'}(M_{\rho'}^2)\left[\mathcal{B}_{\rho'\to\omega\pi^0}\left(\frac{p_\omega(s)}{p_\omega(M_{\rho'}^2)}\right)^3+ (1-\mathcal{B}_{\rho'\to\omega\pi^0})\frac{M_{\rho'}^2}{s}\left(\frac{p_\pi(s)}{p_\pi(M_{\rho'}^2)}\right)^3\right], \quad (6)$$

where the coupling constant $g_{\omega\rho\pi}/M_\omega$ is taken to be 17 GeV^{-1}, which is the fitted value using three different fitting schemes in Ref. [14]. This value is consistent with the experimental values derived from $\omega\to\pi^0\gamma$, $\rho\to\pi^0\gamma$ and $\omega\to\rho\pi\to\pi^+\pi^-\pi^0$ decays, and theoretical estimates based on the QCD sum rules [15–17].

In the above treatment, it is assumed that the dominant $I=1$ background is given by the ρ and ρ' states, for which a relative phase angle is considered:

$$\mathcal{M}_{fi}^{I=1}=\mathcal{M}_{fi}^{a}+\mathrm{e}^{\mathrm{i}\delta_1}\mathcal{M}_{fi}^{b}, \quad (7)$$

where $\delta_1=180°$ is applied as a constructive phase between ρ and ρ' terms in Eq. (7).

2.2 $I=0$ transitions

As pointed out earlier, the isospin-violating $\phi\omega\pi^0$ coupling can occur via the following processes: i) EM transitions through the $s\bar{s}$ annihilation; ii) OZI-rule-evading transitions through intermediate kaon loops; iii) State mixings such as $\phi-\omega-\rho^0$ and $\pi^0-\eta$. We shall discuss these mechanisms in detail as follows.

2.2.1 $I=0$ EM transitions in VMD model

Both ω and ϕ meson can contribute to this amplitude except that ω contributes to the background as illustrated by Fig. 1(c) and (d). We can also factorize out the transition amplitude as the following:

$$\mathcal{M}_{fi}^{\text{EM}-I=0} = (\mathcal{M}_{fi}^{\text{c}-\rho}+\mathrm{e}^{\mathrm{i}\delta_2}\mathcal{M}_{fi}^{\text{d}-\rho})+ \mathrm{e}^{\mathrm{i}\delta_1}(\mathcal{M}_{fi}^{\text{c}-\rho'}+\mathrm{e}^{\mathrm{i}\delta_2}\mathcal{M}_{fi}^{\text{d}-\rho'}), \quad (8)$$

where the detailed expressions for $\mathcal{M}$ can be found in Ref. [11] in the VMD model. In the calculation we fix $\delta_2=0°$ as given by the effective Lagrangians, while $\delta_1=180°$ is required as a constructive phase between the transitions mediated by ρ and ρ' in Fig. 1 (c) and (d).

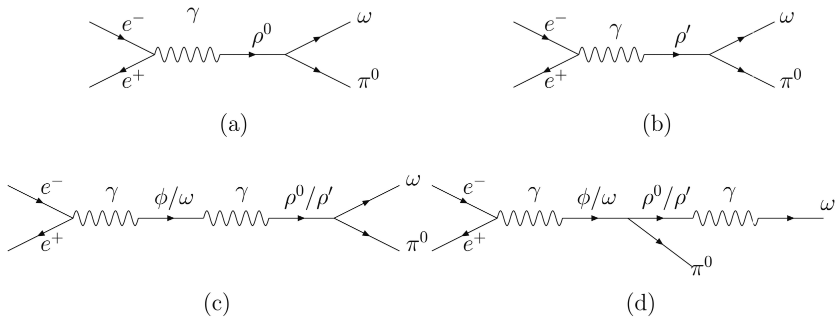

Fig. 1. The schematic diagrams for $I=1$ [(a) and (b)] and $I=0$ EM transitions [(c) and (d)].

2.2.2 $I=0$ transitions via intermediate meson loops

The contributions from the intermediate meson loops are correlated with the state mixings in the next subsection. The transitions can be demonstrated by Fig. 2(a)-(d) as the t-channel processes, while the ϕ-ρ^0 mixing can be recognized via Fig. 2(e) and (f) as the s-channel. As explained earlier, the t-channel strong isospin violation arises from the incomplete cancellations between the charged and neutral kaon loops since they have slightly different masses. In another word, if the charged and neutral K (K^*) mesons have the same mass, their amplitudes will exactly cancel out and the isospin would be conserved. More essentially, it can be recognized that the charged and neutral kaon mass differences originate from the chiral symmetry dynamic breaking which leads to $m_d > m_u$.

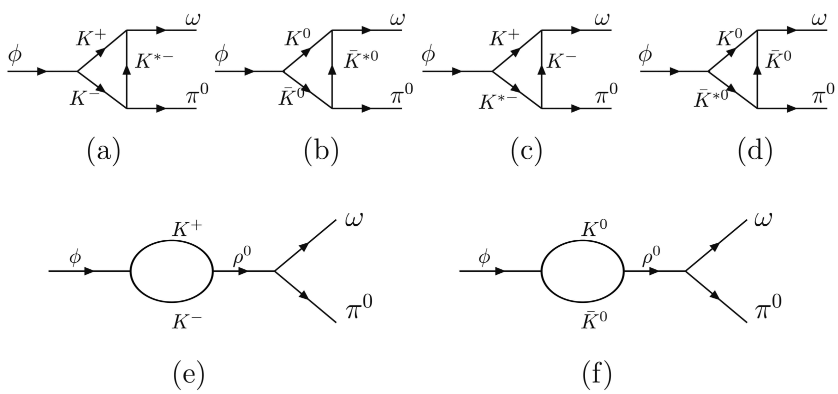

Fig. 2. The transition mechanisms for $\phi\to\omega\pi^0$ via t-channel [(a)-(d)] and s-channel transitions [(e) and (f)].

The transition amplitude for $e^+e^-\to\phi\to\omega\pi^0$ via an intermediate meson loops can be expressed as:

$$\mathcal{M}_{fi}=\bar{v}^{(s')}(p'_e)(-ie\gamma^\rho)u^s(p_e)\frac{-ig_{\rho\sigma}}{s}\frac{eM_\phi^2}{f_\phi}\times \frac{i\varepsilon_\phi^\sigma}{s-M_\phi^2+i\Gamma_\phi(s)\sqrt{s}}\int\frac{d^4p_2}{(2\pi)^4}\sum_{K^*pol}\frac{T_1T_2T_3}{a_1a_2a_3}\mathcal{F}(p_2^2). \quad (9)$$

where the vertex functions for $K\bar{K}(K^*)$ are

$$\begin{cases} T_1 \equiv ig_1(p_1-p_3)\cdot\varepsilon_\phi \\ T_2 \equiv \dfrac{ig_2}{M_\omega}\varepsilon_{\alpha\beta\mu\nu}p_\omega^\alpha\varepsilon_\omega^\beta p_2^\mu\varepsilon_2^\nu, \\ T_3 \equiv ig_3(p_\pi+p_3)\cdot\varepsilon_2 \end{cases}$$

where g_1, g_2, and g_3 are the coupling constants at the meson interaction vertices. The four vectors, p_ϕ, p_ω, and p_{π^0} are the momenta for the initial ϕ and final state ω and π meson; The four-vector momentum, p_1, p_2, and p_3 are for the intermediate mesons, respectively, while $a_1=p_1^2-m_1^2, a_2=p_2^2-m_2^2$, and $a_3=p_3^2-m_3^2$ are the denominators of the propagators of intermediate mesons.

The vertex functions for the $K\bar{K}^*(K)+$c.c. loop are

$$\begin{cases} T_1 \equiv \dfrac{if_1}{M_\phi}\varepsilon_{\alpha\beta\mu\nu}p_\phi^\alpha\varepsilon_\phi^\beta p_3^\mu\varepsilon_3^\nu\ , \\ T_2 \equiv if_2(p_1-p_2)\cdot\varepsilon_\omega\ , \\ T_3 \equiv if_3(p_\pi-p_2)\cdot\varepsilon_3\ . \end{cases}$$

where $f_{1,2,3}$ are the coupling constants.

Similarly, we have vertex functions for the intermediate $K\bar{K}^*(K^*)+$c.c. loop:

$$\begin{cases} T_1 \equiv \dfrac{ih_1}{M_\phi}\varepsilon_{\alpha\beta\mu\nu}p_\phi^\alpha\varepsilon_\phi^\beta p_3^\mu\varepsilon_3^\nu, \\ T_2 \equiv \dfrac{ih_2}{m_2}\varepsilon_{\alpha'\beta'\mu'\nu'}p_2^{\alpha'}\varepsilon_2^{\beta'}p_\omega^{\mu'}\varepsilon_\omega^{\nu'} \\ T_3 \equiv \dfrac{ih_3}{m_3}\varepsilon_{\alpha''\beta''\mu''\nu''}p_2^{\alpha''}\varepsilon_2^{\beta''}p_3^{\mu''}\varepsilon_3^{\nu''} \end{cases}$$

where $h_{1,2,3}$ are the coupling constants. In the above three kinds of vertex functions, the coupling constants are determined via experimental value and $SU(3)$ relations [10, 12, 18].

The form factor $\mathcal{F}(p^2)$, which takes care of the off-shell effects of the exchanged particles and kills the divergence of the loop integrals, is usually parameterized as

$$\mathcal{F}(p^2)=\left(\frac{\Lambda^2-m_{\rm ex}^2}{\Lambda^2-p^2}\right)^n, \tag{10}$$

where $n=0,1,2$ correspond to different treatments of the loop integrals. In the present work, we only consider the monopole form factor, i.e. $n=1$. The cut-off energy Λ is parameterized as:

$$\Lambda=m_{\rm ex}+\alpha\Lambda_{\rm QCD}, \tag{11}$$

where we fix $\Lambda_{\rm QCD}=220$ MeV and α is a tunable parameter; $m_{\rm ex}$ is the mass of exchanged meson.

2.2.3 $I=0$ transitions via ϕ-ρ^0 and ω-ρ^0 strong mixings

The s-channel transitions in Fig. 2(e) and (f) give rise to the ϕ-ρ^0 and ω-ρ^0 mixings. With the effective Lagrangians, we can also calculate their contributions to the ϕ excitations. The mixing effect cannot be significant since the nonvanishing amplitudes are also arising from the incomplete cancellations between the charged and neutral meson loops.

Taking into account the charge-neutral term, the amplitude can be written as

$$\begin{aligned}\mathcal{M}_{fi} &= \bar{v}(p_{\rm e^+})(-{\rm i}e\gamma^f)u(p_{\rm e^-})\times \\ &\quad \frac{1}{s(s-M_\phi^2+{\rm i}\Gamma_\phi(s)\sqrt{s})}\frac{eM_\phi^2}{f_\phi}\times \\ &\quad \epsilon_{\phi\rho}\frac{g_{\omega\rho\pi}}{M_\omega}\varepsilon_{\rm efgh}p_\pi^e p_\omega^g\varepsilon_\omega^h ,\end{aligned} \tag{12}$$

where $\epsilon_{\phi\rho}$ is the strong isospin-violating coupling strength between ϕ and ρ^0,

$$\begin{aligned}\epsilon_{\phi\rho} &\equiv \frac{1}{6\pi\sqrt{s}D_\rho}[g_{\phi{\rm K^+K^-}}g_{\rho{\rm K^+K^-}}P^3_{\rm K^+K^-}(s)+ \\ &\quad g_{\phi{\rm K^0\bar{K}^0}}g_{\rho{\rm K^0\bar{K}^0}}P^3_{\rm K^0\bar{K}^0}(s)],\end{aligned} \tag{13}$$

where $D_\rho\equiv D_\rho(s)=M_\rho^2-s-{\rm i}\sqrt{s}\Gamma_\rho(s)$ and $P_{\rm K^+K^-}$ and $P_{\rm K^0\bar{K}^0}$ are the three-vector momentum of the charged and neutral kaons, respectively. Note that there exists a sign between $g_{\rho{\rm K^+K^-}}$ and $g_{\rho{\rm K^0\bar{K}^0}}$ which brings cancellation between those two terms on the right-hand side of Eq. (13).

At the mass of the ϕ meson, we obtain $\epsilon_{\phi\rho}=(9.51-{\rm i}3.31)\times10^{-4}$ as an effective strong isospin-violating coupling for $\phi\to\rho^0$. This result can be compared with the intermediate meson transition in Eq. (2.10) of Ref. [19] apart from factor D_ρ, while the EM part has been contained in the EM transition amplitudes.

The ω-ρ^0 strong mixing occurs only via intermediate charged pion loop transition. The transition amplitude is similar to that for ϕ-ρ^0 mixing, from which the strong isospin-violating coupling strength can be also defined,

$$\epsilon_{\omega\rho}\equiv\frac{1}{6\pi\sqrt{s}D_\rho}g_{\omega\pi^+\pi^-}g_{\rho\pi^+\pi^-}P^3_{\pi^+\pi^-}(s). \tag{14}$$

At the mass of ϕ meson, we obtain $\epsilon_{\omega\rho}=(13.7-{\rm i}4.8)\times10^{-3}$, which is larger than that $\epsilon_{\phi\rho}$. However, we note in advance that the ω-ρ^0 mixing effects are negligibly small at the ϕ mass.

3 Calculation results

In the numerical study, we adopt resonance masses and widths for ω, ρ^0 from PDG [12], while the coupling constants are either determined by experimental data or $SU(3)$ symmetry [11]. We then have only three parameters to be determined by the KLOE data for $e^+e^-\to\omega\pi^0$, i.e. a phase angle $\delta_{\rm L}$ in Eq. (1), the form factor parameter α, and the total width $\Gamma_{\rho'}$ for ρ'. Two fits are carried out as an investigation of the parameter space. In Fit-I, we fix the phase angle $\delta_{\rm L}=-90°$ while leave α and $\Gamma_{\rho'}$ to be determined by the data. In Fit-II, we free these three parameters to let them be fitted by the data. In Table. 1, the fitted parameters are listed.

Table 1. The parameters fitted in Fit-I and Fit-II schemes.

para.	$\delta_{\rm L}$	α	$\Gamma_{\rho'}$/MeV	χ^2/d.o.f
Fit-I	$-90.0°$ (fixed)	1.125 ± 0.052	674 ± 6	5.71
Fit-II	$-111.6°\pm2.3°$	1.244 ± 0.051	683 ± 6	0.54

Comparing Fit-I with Fit-II, it shows that the relative phase angle between the EM and strong isospin violation amplitudes are important to improve the fitting results. Also, we find very broad widths for ρ'. This could be reasonable since the effective width contains contributions from all ρ resonances apart from the $\rho^0(770)$.

The extracted branching ratios from these two fits are listed in Table 2. They are compared with the PDG [12] and KLOE results [1, 2]. It shows that the ϕ-ρ^0 strong mixing is relatively small and independent of those parameters. Therefore, it keeps the same for both fits and contributes an exclusive branching ratio of 0.37×10^{-5}. The EM amplitudes will depend on the ρ′ width, which leads to small differences between these two fits. We then notice that significant differences between these two fits arise from the meson loop contributions. In Fit-I, the loop contributions constructively interfere with other transitions and lead to a relatively larger branching ratio, $BR_{\phi\to\omega\pi^0}=4.29\times10^{-5}$, while in Fit-II the loop transition amplitude has a destructive effect and gives $BR_{\phi\to\omega\pi^0}=2.83\times10^{-5}$. This is a novel feature arising from the precise data [2].

Table 2. Branching ratios for $\phi\to\omega\pi^0$ extracted from our model with two different fitting schemes. Experimental data [1, 2, 12] and exclusive branching ratios from EM, t-channel meson loop transitions, and s-channel ϕ-ρ^0 mixing are also listed.

$BR(\times10^{-5})$	EM	meson loop	ϕ-ρ^0 mixing	total	PDG [12]	Exp [1]	Exp [2]
Fit-I	2.95	0.93	0.37	4.29	$5.2^{+1.3}_{-1.1}$	5.63 ± 0.70	4.4 ± 0.6
Fit-II	2.97	1.14	0.37	2.83			

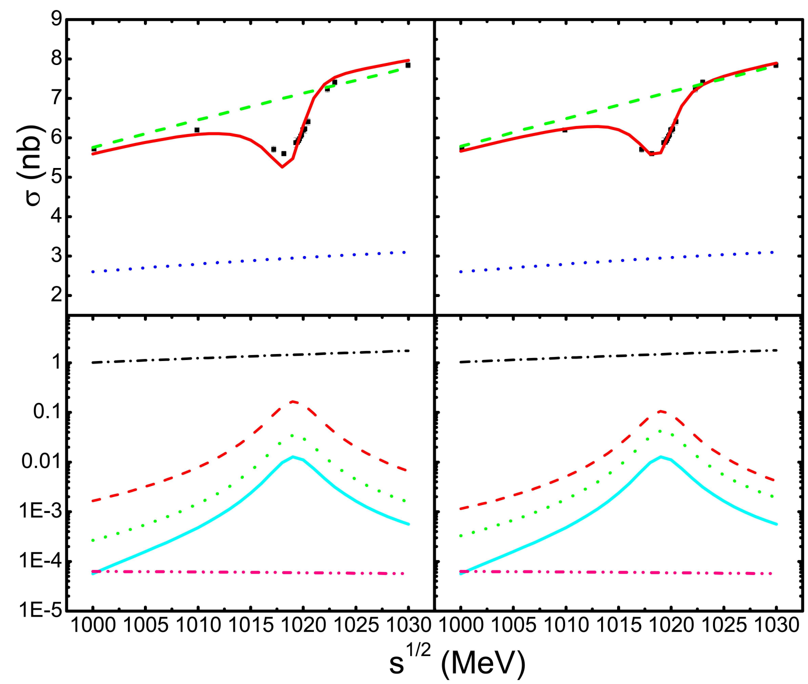

Fig. 3. The $\sqrt{s}$-dependence of the total cross section for $e^+e^-\to\omega\pi^0$ fitted in Fit-I (left) and Fit-II (right). The data are from KLOE measurement [2]. In the lower panels, the dotted curves denote the exclusive t-channel meson loop contributions, the solid lines denote the contributions from the ϕ-ρ^0 mixing, the dot-dot-dashed lines denote the contributions from the ω-ρ^0 mixing, while the dashed ones for the inclusive cross sections for ϕ excitations (EM plus strong isospin violation). The dot-dashed lines stand for cross sections from ρ′(1450) with fitted total widths. In the upper panels, the dotted lines denote the contributions from the ρ meson, while the dashed lines are for the inclusive contributions from background including the dominated $I=1$ component (ρ plus ρ′(1450)) and a small $I=0$ ω excitation. The solid curves are the full model results.

In Fig. 3, we plot the cross sections from different transitions. The following points can be learned from the fitting results:

i) The extracted branching ratio is very sensitive to the lineshape of the ϕ meson dip. This raises questions on the theoretical input in the data analysis. Although such a sensitivity may reflect some model-dependent aspects of this approach, we give cautions to possible uncertainties with the extracted branching ratio from both experiment and theory.

ii) The side-band cross sections are important for determining the background contributions. As shown by the solid curve for the full calculation, at the energies away from the ϕ mass, the contributions from the ϕ excitation die out quickly, and the cross sections are dominated by the $I=1$ components. This is also related to the large values for the extracted ρ′ width. Perhaps, more detailed modelling for the

$I = 1$ component is needed.

iii) Cautions should also be given to the understanding of the non-$\omega\pi^0$ background which will contribute to the 4π final state as studied in experiment [2].

iv) Our calculations show that the ω-ρ^0 mixing effects are negligibly small at the ϕ mass region as illustrated by the dot-dot-dashed curved in the lower panels of Fig. 3. Also, we mention that the contributions from the $\eta-\pi^0$ is small [4] and we neglect it in this work.

v) By defining the background cross section $\sigma_0(\sqrt{s})$ (from $I = 1$ transitions and $I = 0$ ω excitation), the full cross section can be parameterized as [20–22]:

$$\sigma(\sqrt{s}) = \sigma_0(\sqrt{s}) \left|1 - Z\frac{M_\phi \Gamma_\phi}{D_\phi}\right|^2, \quad (15)$$

where M_ϕ and Γ_ϕ are the ϕ mass and width and $D_\phi = M_\phi^2 - s - \mathrm{i}\sqrt{s}\Gamma_\phi$ is the inverse propagator of the ϕ meson; Z is a complex interference parameter that equals to the ratio of ϕ excitation amplitude to the background terms and describes the energy evolution of their relative phase. Our model gives the real and imaginary part of this complex quantity as follows [11]:

$$\text{Fit-I}: (0.107 \pm 0.005,\ -0.110 \pm 0.009), \quad (16)$$

$$\text{Fit-II}: (0.065 \pm 0.002,\ -0.103 \pm 0.005)\ , \quad (17)$$

which are compatible with the experimental results [1, 20–22].

4 Summary

The precise measurement of the ϕ excitation in $e^+e^- \to \omega\pi^0$ [2] as a consequence of interferences between the $I = 1$ and $I = 0$ components in the transition amplitudes provides an opportunity to study the isospin violation mechanisms at low energies. We investigate this process by quantifying the isospin violations in both EM and strong transitions. The $I = 1$ and $I = 0$ EM contributions are studied in the VMD model, while the $I = 0$ strong isospin violating process is described by the t-channel OZI-rule-evading intermediate-mesons-exchange loops and s-channel ϕ-ρ^0 mixing.

The study shows that the cross section of $e^+e^- \to \omega\pi^0$ has evident width-dependence on the ρ' which contributes to the $I = 1$ transition amplitudes. We also find that the extracted branching ratio for $\phi \to \omega\pi^0$ is very sensitive to the line shape of the cross sections in the vicinity of ϕ excitation and the background estimate. Our result turns to be smaller than that given by Ref. [2]. This signals difficulties in extracting the tiny $\phi \to \omega\pi^0$ branching ratio in both experiment and theory.

The OZI-rule-evading transitions via intermediate meson loops provide a natural solution for the ϕ meson non-$K\bar{K}$ decays. Such a mechanism is also found important in heavy quarkonium decays such as the $\psi(3770)$ non-$D\bar{D}$ decays [23]. We expect further experimental results from the ϕ factory and τ-charm factory would help clarify many long-standing questions in the strong QCD sector [24].

References

1 Ambrosino F et al (KLOE collaboration). arXiv: 0707.4130 [hep-ex]

2 Ambrosino F et al (KLOE collaboration). Phys. Lett. B, 2008, **669**: 223 [arXiv:0807.4909 [hep-ex]]

3 Okubo S. Phys. Lett., 1963, **5**: 1975; Zweig G. In: Development in the Quark Theory of Hadrons. Edited by Lichtenberg D B, Rosen S P. Massachusetts: Hadronic Press. 1980; Iizuka J. Prog. Theor. Phys. Suppl., 1966, **37**: 38

4 Bramon A. Phys. Rev. D, 1981, **24**: 1994

5 Donoghue J F, Holstein B R, Wyler D. Phys. Rev. Lett., 1992, **69**: 3444

6 Ametller L, Ayala C, Bramon A. Phys. Rev. D, 1984, **30**: 674

7 Coon S A, McKellar B H J, Scadron M D. Phys. Rev. D, 1986, **34**: 2784

8 Coon S A, R. C. Barrett R C. Phys. Rev. C, 1987, **36**: 2189

9 Genz H, Tatur S. Phys. Rev. D, 1994, **50**: 3263

10 LI G, ZHAO Q, ZOU B S. Phys. Rev. D, 2008, **77**: 014010 [arXiv:0706.0384 [hep-ph]]

11 LI G, ZHANG Y J, ZHAO Q. J. Phys. G, 2009, **36**: 085008 [arXiv:0803.3412 [hep-ph]]

12 YAO W M et al (Particle Data Group). J. Phys. G, 2006, **33**: 1

13 Bauer T, Yennie D R. Phys. Lett. B, 1976, **60**: 169

14 Akhmetshin R R et al (CMD-2 collaboration). Phys. Lett. B, 2003, **562**: 173 [arXiv:hep-ex/0304009]

15 Eletsky V L, Ioffe B L, Kogan Y I. Phys. Lett. B, 1983, **122**: 423

16 Narison S, Paver N. Z. Phys. C, 1984, **22**: 69

17 Lublinsky M. Phys. Rev. D, 1997, **55**: 249 [arXiv:hep-ph/9608331]

18 Tornqvist N A. Annals Phys., 1979, **123**: 1

19 Achasov N N, Kozhevnikov A A. Int. J. Mod. Phys. A, 1992, **7**: 4825

20 Achasov M N et al. Phys. Lett. B, 1999, **449**: 122 [arXiv:hep-ex/9901020]

21 Aulchenko V M et al. J. ExP. Th. Phys., 2000, **90**: 927

22 Achasov M N et al. Nucl. Phys. B, 2000, **569**: 158 [arXiv:hep-ex/9907026]

23 ZHANG Y J, LI G, ZHAO Q. Phys. Rev. Lett., 2009, **102**: 172001 [arXiv:0902.1300 [hep-ph]]

24 Asner D M et al. Physics at BES-III. Edited by Chao K T, Wang Y F. Int. J. of Mod. Phys. A, 2009, **24** Supplement 1 [arXiv:0809.1869]